Journal of
Nanoscience and Nanotechnology
Vol. 8, 1–6, 2008

Formation of Copper Nanowires by Electroless Deposition Using Microtubules as Templates

K. Valenzuela[1], S. Raghavan[1], P. A. Deymier[1,*], and J. Hoying[2]

[1] *Department of Materials Science and Engineering, The University of Arizona, Tucson, AZ 85721, USA*
[2] *Biomedical Engineering Program GIDP, The University of Arizona, Tucson, AZ 85721, USA*

Microtubules (MTs) are self-assembling, protein-based, tubular structures several micrometers long with outer and inner diameters of 25 nm and 15 nm, respectively. This aspect ratio makes MTs ideal templates for producing nanowires for applications such as electrical nano-interconnects. MTs are poorly conductive and their use as interconnects necessitates their metallization. We report a process for metallization of MTs with copper using a biologically benign electroless deposition chemistry consisting of copper sulfate solution containing acetic acid as a complexant and ascorbic acid as reducing agent. The pH of the plating bath is controlled such that copper metallization occurs without disassembling the MTs. Electron microscopic characterization of the morphology and dimensions of the copper nanowires shows that metallization for approximately 1 minute produces a uniform nanowire with an average diameter of approximately 15 nm, suggesting that metallization is initiated selectively from the MT inner core.

Keywords: Copper Nanowires, Electrolee Deposition, Characterization.

RESEARCH ARTICLE

1. INTRODUCTION

Self-assembly of biomolecular templates followed by subsequent metallization is emerging as a potentially low-cost, bottom-up alternative approach to the top-down, wavelength-limited lithography methods currently used in microelectronic manufacturing. A variety of biological templates have already been shown to form nanowires through metallization processes. These include, for example, DNA metallized with silver[1] or palladium,[2] viruses as the substrate for the plating of nickel, cobalt[3,4] or conjugation with platinum nanoparticles,[5] and proteins structures such as microtubules (MTs) coated with nickel or cobalt[6,7] or gold.[8]

MTs are naturally formed proteinaceous tubular structures, 25 nm and 15 nm in outer and inner diameter, respectively, and up to many microns in length. They are biopolymers assembled from two related protein monomers; α and β-tubulins. In the presence of guanosine triphosphate (GTP), these tubulin monomers form GTP-bound tubulin heterodimers, which self-assemble into the MT structure. The structure of MT consists of a two-dimensional helical lattice composed of 13 protofilaments formed from the tubulin heterodimers and aligned along the principal axis of the tubule. Dynamic instability is an intrinsic property of MTs.[9] For tubulin concentrations above a critical value, C_c, MTs self-assemble. Below the C_c, MTs depolymerize.[10] The stability of MTs in solution (i.e., C_c) is dependent on several factors, such as, temperature and chemistry. Additionally, small molecules such as taxol are well known to have a stabilizing effect; microtubule-associated proteins (MAP) that bind to the exterior surface of the microtubules favor polymerization.[11]

Nickel and cobalt metallization of MTs has been typically attempted using a two-step process[6,7] consisting of surface activation with a noble metal such as Pd or Pt, which serves as a catalyst for the second step, followed by the electroless deposition of the desired metal. MTs have also been metallized with Pd using a palladium salt. The proposed mechanism for these two step electroless approaches is the interaction of the ions with histidine groups on the external surface of the tubule resulting in the deposition of palladium nanoparticles.[12] Another study has also shown that MAP-stabilized MTs are a more viable option for nickel metallization.[13] In all of these studies, metallization of the MTs did not show selectivity with respect to the inner and outer surfaces of the tubule. Interestingly, such selectivity was observed for the metallization of tubular tobacco mosaic virus presumably because of the presence of functional groups that differed on the inside and outside surfaces.[3,4]

*Author to whom correspondence should be addressed.

The main objective of the work reported in the present paper is to develop a process for metallizing MTs with copper. Copper is currently the interconnect metal of choice in integrated circuits due to its low electrical resistivity. While there is currently no published work on the copper plating of microtubules, there is one report on the copper plating of bolaamphiphile nanotubes.[14, 15] The metallization mechanism in that study was determined to be the binding of ions to available amine groups and reduction of these ions to metal in the plating baths.[14] The amine groups in the bolaamphiphiles peptide monomers play a crucial role in the binding of copper ions to the nanotube as shown by Banerjee et al.[14] who immobilized a histidine-rich peptide onto the amine groups by hydrogen bonding. Histidine is known to have high affinity to ions of metals such as copper.[15]

We report on the development of a biocompatible electroless copper deposition bath chemistry for selective copper metallization of MT. The bath consists of a copper sulfate solution containing acetic acid as a complexant and ascorbic acid as the reducing agent. Since copper plating takes place at pH = 4, we have investigated the stability of various MT solutions at low pH and shown that the kinetics of copper ion reduction exceeds that of MT disassembly. Finally, electron microscopic characterization of metallized MTs suggests that copper reduction occurs initially (and preferentially) at the inner core surface of MTs.

2. METHODS

2.1. Formation of MT

Microtubules were formed from tubulin solutions with and without MAP. Low purity, MAP-rich tubulin (~30% MAPs) and high purity tubulin (>99% tubulin monomers) were used for the formation. These tubulin proteins were isolated from bovine brain (Cytoskeleton, Inc.) and stored at −70 °C in G-PEM buffer (pH 6.8). *In-vitro* MT assembly was performed in a buffer consisting of PEM80 buffer (80 mM PIPES, 1 mM EGTA, 4 mM $MgCl_2$, using KOH to adjust the pH to 6.9), 10 mM of GTP and 10 mM of taxol. Tubulin was added (final concentration of tubulin was 1.5 mg/ml) to this buffer to start polymerization. Polymerization of the MTs was completed after rotating the solution in an incubator at a low speed of 15 rpm for 30 minutes at 37 °C.

2.2. Immunolabeling of MTs

Microtubules were visualized by fluorescence immunolabeling. MTs were immobilized on poly-L-lysine coated glass coverslips for 20 to 25 minutes prior to exposure to a monoclonal anti-β-tubulin antibody (Sigma Inc.) for 30 minutes. Immobilized MTs were incubated with a secondary antibody labeled with Cy3 directed against mouse IgG for 30 minutes. MTs were washed with PBS buffer (Phosphate-buffered saline with a pH of 7.4) between and after each step. Immunolabeled MTs were visualized with an IM71 Inverted epifluorescence microscope (Olympus Inc.) using a 100× fluor objective.

2.3. Investigation of Stability of MTs at Low pH

The procedure for the testing of the stability of MTs in acidic conditions was as follows. MTs were exposed to a solution at pH 4 for different time increments. A control was established by diluting the MT stock solution with PEMTAX (500:1 ratio of PEM80 buffer to taxol) at pH 6.9 and immediately adding a 2% glutaraldehyde solution (in PEM80) to the mixture to arrest MT polymerization dynamics. The overall dilution of the MTs in buffer and glutaraldehyde mixture was 1:50. The purpose of the glutaraldehyde was to fix the MTs. Another batch of MTs was diluted 1:50 in a 0.02 M acetic acid to 0.02 M ascorbic acid solution with an adjusted pH value of 4.0 using KOH. This solution is the copper plating solution with the copper sulfate component absent. The purpose was to determine if acetic acid and ascorbic acid had any adverse effects on the MTs. After 1, 3, and 5 minutes, MT assembly and disassembly dynamics were arrested by the addition of glutaraldehyde. This procedure was carried out for both kinds of MTs (pure and MAP stabilized). The samples were then immunolabeled for observation in an epifluorescence microscope as described above.

2.4. MT Metallization and Characterization

The first step in the procedure for copper metallization was the preparation of the copper plating solution, which was added to the MT stock solution in a ratio of 25:1. After a predetermined time period (1 to 4 minutes), a 2% glutaraldehyde solution in PEM80 was added to the solution containing the metallized MTs. Excess ions in the solution were then removed by dialysis. The dialyzed solution containing metallized MTs was then centrifuged for 10 minutes at 13 rpm. This step served to concentrate the metallized MTs at the bottom of the tube so they could be extracted and dried onto a carbon coated nickel grid (Ted Pella, Inc.). Images of metallized microtubules were then taken with a Hitachi H8100 Transmission Electron Microscope (TEM). The presence of the copper film on the microtubules was confirmed using Thermo-Noran Digital Imaging/energy-dispersive spectroscopy (EDS) capabilities of the TEM.

3. RESULTS

3.1. Development of Biologically Benign Electroless Copper Deposition Chemistry

The basic components of an electroless plating bath are a metal salt (source of cation), and a reducing agent. Other

additives may include complexing agents and stabilizers. Complexing agents are used to prevent precipitation of metal salts and limit the free metal ions in solution whereas stabilizers control the plating rate and prevent decomposition of solution.

Electroless deposition of copper onto MTs using commercially available plating baths poses a challenge as these baths often contain formaldehyde as a reducing agent; a substance toxic to MTs. Additionally, commercial plating conditions require alkaline pH values (11.5 to 13) at elevated temperatures of 55 °C to 70 °C.[16] Under these conditions, MTs are unstable and disassemble readily.

Copper sulfate was used as the metal ion source for the plating chemistry. Several reducing agents were investigated but ascorbic acid was chosen as the optimum reducing agent. Ascorbic acid is known to reduce silver chloride to silver metal[17] as well as Ce(IV).[18] The reduction of copper (II) ions to copper (I) ions with ascorbic acid has been widely studied in the presence of oxygen, halide anions, and other elements.[19] The standard reduction potential (E^0) of ascorbic acid varies with pH, with values of -0.127 and -0.34 V for pH values of 4 and 7, respectively.[17] With a standard reduction potential of ($Cu^{+2} + 2e = Cu$) 0.34 V for cupric ions, it is thermodynamically feasible to reduce copper ions to copper metal by ascorbic acid at acidic pH values. Additionally, acetic acid was chosen as the complexing agent due to its buffering capability when mixed with acetate ions. From the Pourbaix diagram in Figure 1, it may be seen that copper ions complex with 1 to 3 molecules of acetic acid. For this reason, the molar concentration of acetic acid was chosen to be 2 times greater than the concentration of the copper sulfate.

Since prior studies have shown that metallization of platinum activated MTs is feasible, platinum was used as the substrate for the initial development of copper plating solutions. The plating chemistry for copper metallization was modified repeatedly to establish a solution that would generate a thin, uniform film of copper at a pH as close to physiological pH as possible. A chemical composition consisting of 0.01 M copper sulfate, 0.02 M acetic acid and 0.02 M ascorbic acid at a pH of 4 was found to produce a uniform copper film onto a Pt foil after 4 minutes. Visually, slight copper deposition was noticed after 90 seconds. XRD analysis confirmed that the film was metallic copper.

The choice of pH for copper plating is very critical. Acidic pH values favor plating but MT stability is favored by neutral pH values. If the kinetics of electroless plating of copper is faster than the disassembly kinetics of MTs at lower pH values, then it is possible to plate the MTs before they may disassemble. Therefore, we also studied the effect of pH on the reduction of copper. A series of experiments was conducted whereby copper was deposited on the surface of Pt wires at pH >4. At a pH greater than 4.3, the formation of copper oxide (cuprite) precipitates was significantly greater than that of metallic copper. Therefore, it was determined that the optimum pH for copper deposition was a pH in the vicinity of 4.

3.2. Stability of MTs at Low pH

Electroless deposition of copper in the presence of acetic and ascorbic acid requires a pH of approximately 4. The kinetics of disassembly of MTs at pH values far from the physiological pH value is not well established. In this section we report results of our investigation on the stability of MTs at pH = 4, which was done to determine if the kinetics of MT disassembly can be made slower than that of the metal deposition. Two types of MTs were considered, namely MT grown from pure tubulin and from MAP-containing tubulin solution.

Figures 2 and 3 show unambiguously that both types of MT preparations (pure and MAP-containing MTs) retain their structural integrity after exposure to an acidic solution with pH = 4 for at least 5 minutes. In both sets of

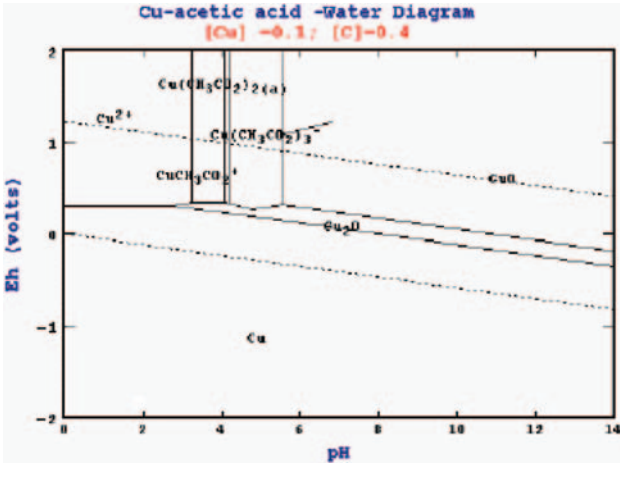

Fig. 1. Pourbaix diagram of copper in acetic acid solutions.

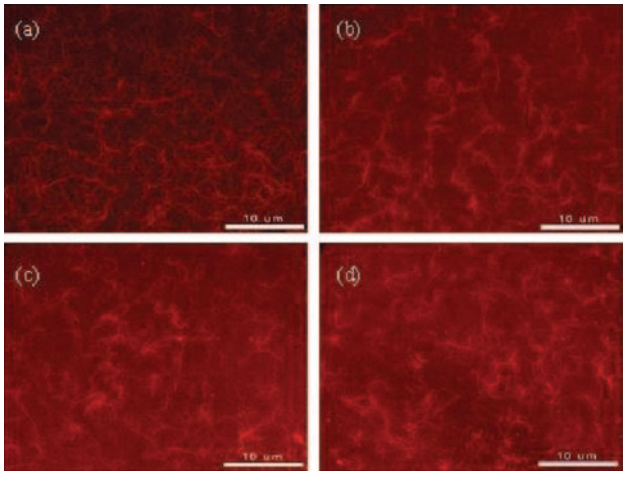

Fig. 2. Fluorescence microscopy images of pure MTs exposed to a solution with a pH of 4. (a) Control (b) after an exposure time of 1 minute, (c) 3 minutes, and (d) 5 minutes.

RESEARCH ARTICLE

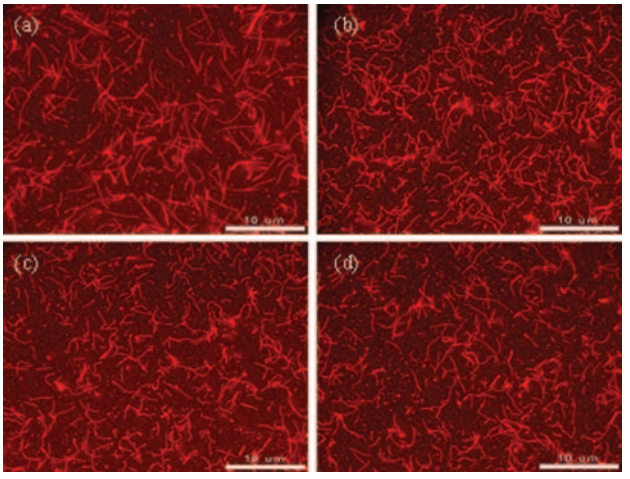

Fig. 3. Fluorescence microscopy images of MAPs stabilized MTs exposed to a solution with a pH of 4. (a) Control (b) after an exposure time of 1 minute, (c) 3 minutes, and (d) 5 minutes.

experiments, the concentration of MTs appears to remain the same but it was also observed that the lengths of the MTs began to decrease slightly after approximately 3 minutes. The facts that pure MTs and MTs with MAPs are stable for more than 5 minutes in acidic solutions at pH = 4, and copper reduction occurs within 4 minutes, suggest that the developed plating formulation may be able to metallize MTs.

3.3. Copper Metallization of MTs

Since pure MTs and MAPs containing MTs exhibited similar disassembly kinetics at pH = 4, all subsequent experiments were conducted with pure MTs. In Figure 4, we present typical TEM images of MTs metallized for 1, 2 and 4 minutes. It may be noticed that the MTs metallized for 4 minutes have non-uniform diameters that range from 13 to 32 nm and have a very rough external surface (Fig. 4(c)). In contrast, the MTs metallized for 1 and 2 minutes (Figs. 4(a and b)) exhibit a much smoother surface with a more uniform diameter along most of the MT lengths. For instance, the diameter of the MTs metallized for 1 minute ranges from 10 to 18 nm.

The presence of the metallic copper was confirmed using the EDS capabilities of the TEM. The EDS spectrum identified C, Cu, and Ni as the major elements. The carbon and nickel peaks are attributed to the TEM grid and copper is the only element identified on the MT surface.

The synthesis of copper nanowires by metallization of MTs is also supported by high-resolution images of a MT metallized for 1 minute shown in Figure 5. The observation of lattice fringes across the MT suggests the presence of crystalline copper.

To quantify the kinetics of copper metallization of MTs, the diameters of the metal nanowires were measured from TEM pictures. For each sample, the diameters of 5 different MTs were measured, approximately every 150 nm

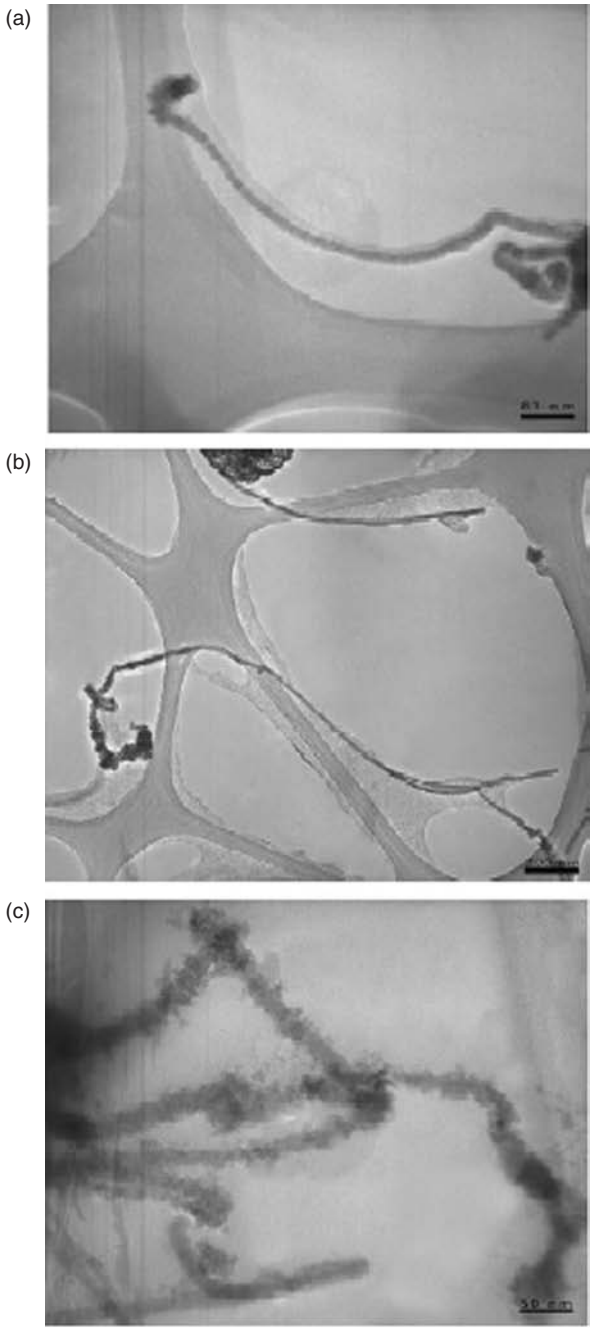

Fig. 4. TEM micrographs of MTs metallized for (a) 1, (b) 2, and (c) 4 minutes. The samples are supported by a carbon coated nickel grid. Note the different scales at the bottom right of the pictures.

along the length of every MT and included regions of large and small diameters. As seen in Figure 4 there are large copper particles that were attached to the ends of some MTs. In this case, the MT diameter was measured up to the region of copper particles. The average diameter of the 5 nanowires formed after 1 minute was determined to be 15.2 nm with a standard deviation of 4.7. The same measurements for the nanowires produced after 2 minutes, yielded an average of 16.8 nm and a standard deviation of 3.0. After four minutes of metallization, the overall

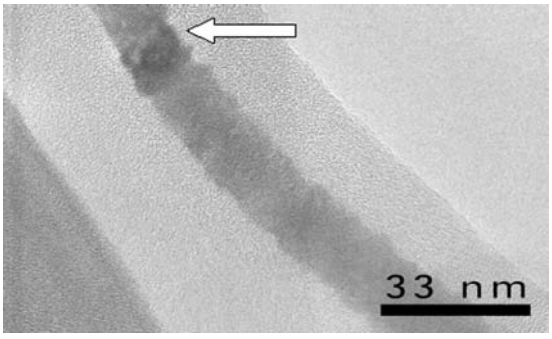

Fig. 5. High resolution image of MT metallized for 1 minute (the arrow points at some of the lattice fringes).

average and the standard deviation were calculated to be 23.9 nm and 6.1, respectively. These average diameter data are plotted as a function of metallization time in Figure 6.

The observation of copper nanowires exhibiting diameters smaller than the outer diameter of the MT template suggests that the metallization occurs preferentially inside the MT and proceeds outward. For the longer time studied (4 min), the metallization reaches the outer surface of the MTs. The uniformity of the copper wire and the lattice fringes observed in the HRTEM images of MTs metallized for 1 min support the monolithic nature of the copper nanowire and rules out the possibility of other processes such as metallization of the outer surface of MTs followed by a collapse of the copper tube into a nanowire with a small diameter. From the results of Figure 6, we estimate that the copper deposition rate during the first minute of metallization is approximately 15.0 nm/min.

The kinetics of MT metallization and the structure of the observed nanowires support a copper deposition mechanism whereby metal reduction is initiated within the inner core of MTs. In a recent *ab-initio* (DFT) computational

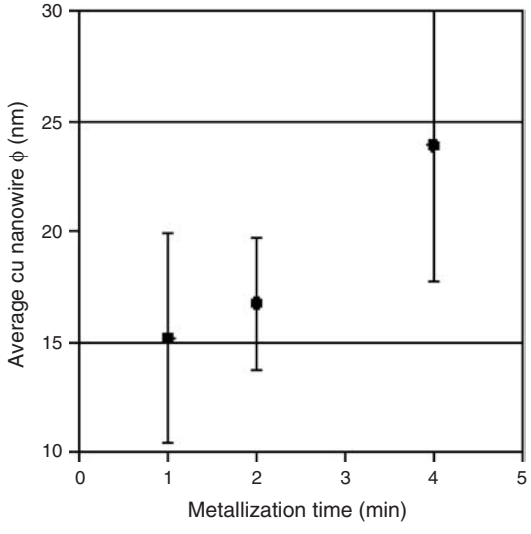

Fig. 6. Average copper nanowire diameter versus MT metallization time. The two horizontal lines illustrate the inner and outer diameters of non-metallized MTs.

study of Cu^{2+} binding to different molecular fragments of MTs, we have shown that a histidine-containing site found on the inner surface of the MT has the highest affinity towards copper ions and, therefore, is the most probable target for initiation of copper metallization.[21] That same study showed another potential histidine metallization site on tubulin which is exposed to the outer MT surface. This outer site histidine has a slightly lower affinity than that of the inner site histidine. However, since the number of metallization sites per tubulin dimer on the inner side of the MT is nearly equal to the number of sites on the outer side, but their density per unit surface is higher due to smaller inner surface in comparison to the outer surface, copper metallization originating from the inner surface may likely be the dominant process.

The histidine amino acid contains an imidazole functional group, which is known to bind to copper strongly. Since the plating chemistry contains acetate ions, copper will be present as a copper acetate complex ion prior to the start of the plating step. The deposition of copper in the interior of the MTs would require that the copper binds to imidazole groups in the inner surface of the MTs. This is feasible if copper-acetate complexes are less stable than the copper-imidazole complexes. To check if this is true, a search of literature was done on the stability of copper ions complexes with imidazole and acetate. Imidazole forms complexes with both Cu(II) and Cu(I) ions. Specifically, imidazole forms four complexes with Cu(II) ions with an overall binding constant ($\sum K_i$) of $10^{12.6}$. Cuprous ions form 1:1 and 1:2 complexes with imidazole with an overall stability constant of 10^{11}. In the case of acetate ions, only cupric ions form complexes; the 1:1 and 1:2 complexes between cupric ions and acetate ions are characterized by log K values of 2.16 and 3.20, respectively. If one considers 1:1 complexes with both ligands, the $Cu(imidazole)^{2+}$ complex is much more stable (by a factor of 10^2) than the $Cu(acetate)^+$ complex, as represented in the following equations:

$$Cu^{2+} + CH_3CO_2^- \rightarrow CuCH_3CO_2^+ \quad \log K_1 = 2.11$$

$$Cu^{2+} + Im \rightarrow CuIm^{2+} \quad \log K_1 = 4.10$$

For the displacement of the acetate ion bound to copper by imidazole, the following equation can be written:

$$CuCH_3CO_2^+ + Im \rightarrow CuIm^{2+} + CH_3CO_2^- \quad \log K^* = 1.99$$

The high value of the equilibrium constant ($\sim$100) for the above reaction indicates that imidazole groups on the interior of MTs can bind to copper acetate complexes with the attendant release of acetate ions.

Based on the available experimental and theoretical results, we can propose a mechanism for the metallization of the inside of the MTs. First, copper ions complexed with acetic acid diffuse through the porous wall of the MT. In the inner core of the MT, the copper-acetate ions bind

RESEARCH ARTICLE

to the imidazole group of histidine residues and copper-acetate is converted to a copper-imidazole complex. Next, ascorbic acid penetrates the MT wall and reduces the copper ions to metallic copper nuclei. These copper nuclei catalyze further copper metallization on the inside of the MT.

4. CONCLUSIONS

In conclusion, we report on a method for selective electroless copper metallization of microtubules. It consists of a solution containing 0.01 M copper sulfate, 0.02 M acetic acid and 0.02 M ascorbic acid. The optimum pH at which rapid copper film formation occurs was found to be 4.0. At this pH, sufficient metallization occurs prior to the disassembly of MTs (which occurs under acidic conditions). Metallization appears to be initiated selectively from the inner core of MTs. This approach enables the use of microtubules as templates for manufacturing copper nanowires with 15 nm diameter.

Acknowledgments: We acknowledge financial support from NSF/NIRT Grant 0303863.

References and Notes

1. E. Braun, Y. Eichen, U. Sivan, and G. Ben-Yoseph, *Nature* 391, 775 **(1998)**.
2. J. Richter, R. Seidel, R. Kirsch, M. Mertig, W. Pompe, J. Plaschke, and H. K. Schackert, *Adv. Mater.* 12, 507 **(2000)**.
3. M. Knez, A. M. Bittner, F. Boes, C. Wege, H. Jeske, and K. Kern, *Nano Lett.* 3, 1079 **(2003)**.
4. M. Knez, M. P. Sumser, A. M. Bittner, C. Wege, H. Jeske, T. P. Martin, and K. Kern, *Adv. Funct. Mater.* 14, 116 **(2004)**.
5. R. J. Tseng, C. Tsai, L. Ma, J. Ouyang, C. S. Ozkan, and Y. Yang, *Nature Nanotech.* 1, 72 **(2006)**.
6. R. Kirsch, M. Mertig, W. Pompe, R. Wahl, G. Sadowski, K. J. Böhm, and E. Unger, *Thin Solid Films* 305, 248 **(1997)**.
7. M. Mertig, R. Kirsch, and W. Pompe, *Appl. Phys. A* 66, S723, **(1998)**.
8. B. A. Diners, M. A. Harmer, and G. Mitchell, US Patent Application, Pub. No: US200410063915A1, April 1 **(2004)**.
9. T. Mitchison and M. Kirschner, *Nature* 312, 237 **(1984)**.
10. H. Lodish, A. Berk, S. L. Zipuski, P. Matsudaira, D. Baltimore, and J. Darnell, Molecular Cell Biology, 4th edn., Freeman, New York **(2000)**.
11. K. Kinoshita, I. Arnal, A. Desai, D. N. Drechsel, and A. A. Hyman, *Science* 294, 1340 **(2001)**.
12. S. Behrens, K. Rahn, W. Habicht, K. J. Böhm, H. Rösner, E. Dinjus, and E. Unger, *Adv. Mater.* 14, 1621 **(2002)**.
13. Yi Yang, B. Constance, P. A. Deymier, J. Hoying, S. Raghavan, and B. J. J. Zelinski, *J. Mater. Science* 39, 1927 **(2004)**.
14. H. Matsui, S. Pan, B. Gologan, and S. H. Jonas, *J. Phys. Chem. B* 104, 9576 **(2000)**.
15. I. A. Banerjee, L. Yu, and H. Matsui, *PNAS* 100, 14678 **(2003)**.
16. Y. Shacham-Diamand, *J. Micromech. Microengr.* 1, 66 **(1991)**.
17. D. Tong and S. Jianjun, Selected Papers of EC&M '96, 8, 48 **(1997)**.
18. K. Chinna Rajanna, Y. Rajeswar Rao, and P. K. Saiprakash, *Indian Journal of Chemistry* 17A, 66 **(1979)**.
19. G. Zhang and H. Chen, *Anal. Sci.* 16, 1317 **(2000)**.
20. K. Hayakawa, S. Minami, and S. Nakamura, *Bull. Chem. Soc. Jpn.* 46, 2788 **(1973)**.
21. B. Trzaskowski, P. A. Deymier, and L. Adamowicz, *J. Mater. Chem.* **(2006)**.

Received: 12 November 2006. Accepted: 13 September 2007.